Erratum: 'Contributions to the geomagnetic secular variation from a reanalysis of core surface dynamics' and 'Assimilation of ground and satellite magnetic measurements: inference of core surface magnetic and velocity field changes'

Barrois, O.; Gillet, N.; Aubert, J.; Hammer, M. D.; Finlay, C. C.; Martin, Y

Published in:
Geophysical Journal International

Link to article, DOI:
10.1093/gji/ggy471

Publication date:
2018

Document Version
Peer reviewed version

Erratum: 'Contributions to the geomagnetic secular variation from a reanalysis of core surface dynamics'† and 'Assimilation of ground and satellite magnetic measurements: inference of core surface magnetic and velocity field changes'‡

†O. Barrois[1], N. Gillet[1] & J. Aubert[2]

‡O. Barrois[1], M.D. Hammer[3], C.C. Finlay[3], Y. Martin[1] & N. Gillet[1]

[1] *Univ. Grenoble Alpes, CNRS, ISTerre, CS 40700 F-38058 Grenoble cedex 9, France.*

[2] *Institut de Physique du Globe de Paris, Sorbonne Paris Cité, Univ. Paris Diderot, CNRS, 1 rue Jussieu, F-75005 Paris, France.*

[3] *Division of Geomagnetism, DTU Space, Technical University of Denmark, Lyngby DK-2800, Denmark.*

Key words: errata, addenda – Core flow – Data assimilation – Error estimation – Stochastic models – Kalman Filter – core dynamics – geomagnetic field modelling – satellite observations

Erroneous statistical estimate of diffusion

We report changes to the calculations presented in the two studies by Barrois et al. (2017) and Barrois et al. (2018) – hereafter referred to as respectively BGA17 and BHF18. Considerations about diffusion in section 2.3 of BGA17 appear to result from a mis-interpretation of the numerical estimates. Let's write $\mathbf{b}$ and $\mathbf{u}$ the vectors containing coefficients defining the projection onto large length-scales of the magnetic and velocity fields at the core-mantle boundary (CMB). The radial induction equation at the CMB (their equation (11)), writes in matrix form

$$d\mathbf{b}/dt = \mathsf{A}(\mathbf{b})\mathbf{u} + \mathbf{e} + \mathbf{d}\,, \tag{1}$$

where vectors $\mathbf{d}$ and $\mathbf{e}$ contain the signature respectively of magnetic diffusion and of (nonlinear) subgrid scale interactions. We realized that the ability to recover $\mathbf{d}$ from (i) observations of $\mathbf{b}$ and $\mathbf{u}$ and (ii) empirical cross-covariances constructed from realizations of the above fields from geodynamo series (their figure 1) is only apparent. It indeed only works for samples that have been used to generate the cross-covariance matrices that enter their equation (18). A linear estimation framework using covariance statistics constructed from a number of samples (as done to estimate diffusion in BGA17) is indeed subject to spuriously good recovery results when tested with any linear combination of these samples. We anticipate that this effect disappears in the limit where the number of samples largely exceeds the dimension of the covariance matrix, which is not the case in our study.

As a consequence, the proposed maps of diffusion, as well as the contribution from diffusion in secular variation (SV) series, are not valid. Furthermore, the vector $\mathbf{e}$ that augments the state vector in BGA17 should account not only for the signature of subgrid scale processes, but also for that of diffusion. We have thus revisited the geophysical results of the two studies using this way of estimating magnetic diffusion at the CMB (BGA17 and BHF18) while (i) discarding the analysis for diffusion, and (ii) replacing, in both the forecast auto-regressive model and the analysis of SV data, the augmented state vector $\left[\mathbf{u}^T\mathbf{e}^T\right]^T$ by $\left[\mathbf{u}^T\mathbf{g}^T\right]^T$ with $\mathbf{g} = \mathbf{e} + \mathbf{d}$. Accordingly, the cross-covariance matrix P_{ee} that enters equation (14) of BGA17 is replaced by $\mathsf{P}_{gg} = E\left((\mathbf{g} - \hat{\mathbf{g}})\,(\mathbf{g} - \hat{\mathbf{g}})^T\right)$, with $\hat{\mathbf{g}} = E(\mathbf{g})$. As in BGA17 and BHF18, cross-covariances are extacted from the Coupled-Earth dynamo (Aubert et al. 2013).

Revised re-analysis from Gauss coefficients data

We first compare a re-analysis similar to that of BGA17 (inverting for diffusion separately from $\mathbf{e}$) with a re-analysis in the configuration where diffusion is accounted for through $\mathbf{g}$. Observations consists, as in BGA17, of MF and SV Gauss coefficients over the period 1955–2020. In both cases we corrected for two mistakes in BGA17 already mentionned in BHF18: a sign error in the background flow, and the omission of off-diagonal elements in P_{ee} (now P_{gg}). All other aspects of the forward and inverse procedure are kept the same (in particular using scaled prior matrices, see configuration D in Table 3 of BGA17). We illustrate below the changes observed between the two re-analyses, with secular variation Gauss coefficient series, core flow Gauss coefficient series and maps at the CMB.

SV Gauss coefficients predictions

We first remind that in the revised configuration, one cannot distinguish anymore between the contributions from $\mathbf{d}$ and $\mathbf{e}$. We see in Figure 1 a slightly larger dispersion for $\mathbf{g}$ than for $\mathbf{e}$, which seems logical given the definition of $\mathbf{g}$. The contribution from $\mathbf{d} + \mathbf{e}$ in the BGA17 configuration generally

encompasses, within the errorbars provided by the ensemble spread, the contribution from $\mathbf{g}$ in the revised configuration of the present erratum. In particular for the axial dipole SV, the revised run indicates that diffusion plus subgrid effects are responsible for a smaller fraction of the dipole decay over the satellite era, while the contribution associated with large length-scale fields is almost constant over the whole time-span, around 8 nT/yr – corresponding to an average contribution from the gyre, as in the scenario by Finlay et al. (2016a).

[Figure 1 about here.]

Core flows

Core flow coefficient series agree reasonably well between the two runs compared here, given the errorbars estimated for the flow models (see Figure 2). Maps of the core motions at the CMB nevertheless show slightly less complexity when the SV contribution from diffusion enters $\mathbf{g}$, as illustrated in Figure 3.

[Figure 2 about here.]

[Figure 3 about here.]

Revised re-analysis from VO and GO data

We also perform revised re-analyses using as data virtual observatories (VO) and ground-based observatories (GO) over the period 1998–2018, as presented in BHF18. We obtain SV predictions (see Figure 4) compatible with the above inversions performed from Gauss coefficient data. In particular we recover a comparable contribution to the dipole decay from the interaction of large length-scale fields. As observed above, the contribution from $\mathbf{e} + \mathbf{d}$ from BHF18 most of the time encompasses, within the ensemble spread, that of obtained in the configuration of the present erratum. Analyses are performed here every 4 months – against 8 months in BHF18, contrary to what they indicate.

[Figure 4 about here.]

While the ensemble spread within the ensemble of flow models is very similar with the two approaches, the ensemble average flow model obtained in the configuration of the present erratum is significantly less energetic towards small length-scales (see Figure 5). The recomputed results suggest coefficients of degree above about 10 are not well resolved. Despite this discrepancy, our revised results lead to similar qualitative conclusions. In particular, we recover the birth of a significant Eastward acceleration under the Eastern equatorial Pacific over the studied satellite era (Figure 6). As in BHF18, the acceleration of the high latitude Westward jet put forward by Livermore et al. (2017) is present: we

witness an increase in magnitude of the ensemble average flow locally up to about 60% over the studied era. As in BHF18, this feature does not appear equatorially symmetric, and does not dominate the acceleration budget over the past 20 yrs. Indeed, the average acceleration also highlights the evolution of (predominantly equatorially symmetric) mid to high latitude eddies in the Pacific hemisphere. The energy is now more evenly distributed betwen the regions around the Estearn and Western meridional branches of the planetary gyre.

[Figure 5 about here.]

[Figure 6 about here.]

Conclusion

We revise the statement on diffusion put forward by BGA17: we do not manage to recover diffusion from geodynamo statistics and the knowledge of the magnetic and velocity fields at large length-scales. We revised the re-analyses presented in BGA17 and BHF18, using a corrected implementation. These lead to qualitatively similar geophysical conclusions – diffusion put aside. We conclude that the augmented state Kalman filter algorithm presented in BGA17, based on cross-covariances derived from geodynamo coefficient series, is robust provided the contribution from diffusion to the SV is accounted for together with subgrid processes (through the above vector $\mathbf{g}$). The revised coefficient series from the re-analysis performed in the present erratum are available at the address `https://geodyn.univ-grenoble-alpes.fr/`.

1 ACKNOWLEDGEMENTS

We are grateful to Loic Huder for computing all models shown in the present erratum. This study is partially supported by the French Centre National d'Etudes Spatiales (CNES) for the study of Earth's core dynamics in the context of the *Swarm* mission of ESA.

REFERENCES

Aubert, J., Finlay, C. C., & Fournier, A., 2013. Bottom-up control of geomagnetic secular variation by the Earth's inner core, *Nature*, **502**(7470), 219–223.

Barrois, O., Gillet, N., & Aubert, J., 2017. Contributions to the geomagnetic secular variation from a reanalysis of core surface dynamics, *Geophys. J. Int.*, **211**(1), 50–68.

Barrois, O., Hammer, M., Finlay, C., Martin, Y., & Gillet, N., 2018. Assimilation of ground and satellite magnetic measurements: inference of core surface magnetic and velocity field changes, *Geophys. J. Int.*, **215**(1), 695–712.

Finlay, C. C., Aubert, J., & Gillet, N., 2016a. Gyre-driven decay of the Earths magnetic dipole, *Nature communications*, **7**, 10422.

Finlay, C. C., Olsen, N., Kotsiaros, S., Gillet, N., & Tøffner-Clausen, L., 2016b. Recent geomagnetic secular variation from Swarm, *Earth, Planets and Space*, **68**(1), 1–18.

Gillet, N., Barrois, O., & Finlay, C. C., 2015. Stochastic forecasting of the geomagnetic field from the COV-OBS. x1 geomagnetic field model, and candidate models for IGRF-12, *Earth, Planets and Space*, **67**(1), 1–14.

Livermore, P. W., Hollerbach, R., & Finlay, C. C., 2017. An accelerating high-latitude jet in Earth's core, *Nature Geoscience*, **10**(1), 62–68.

LIST OF FIGURES

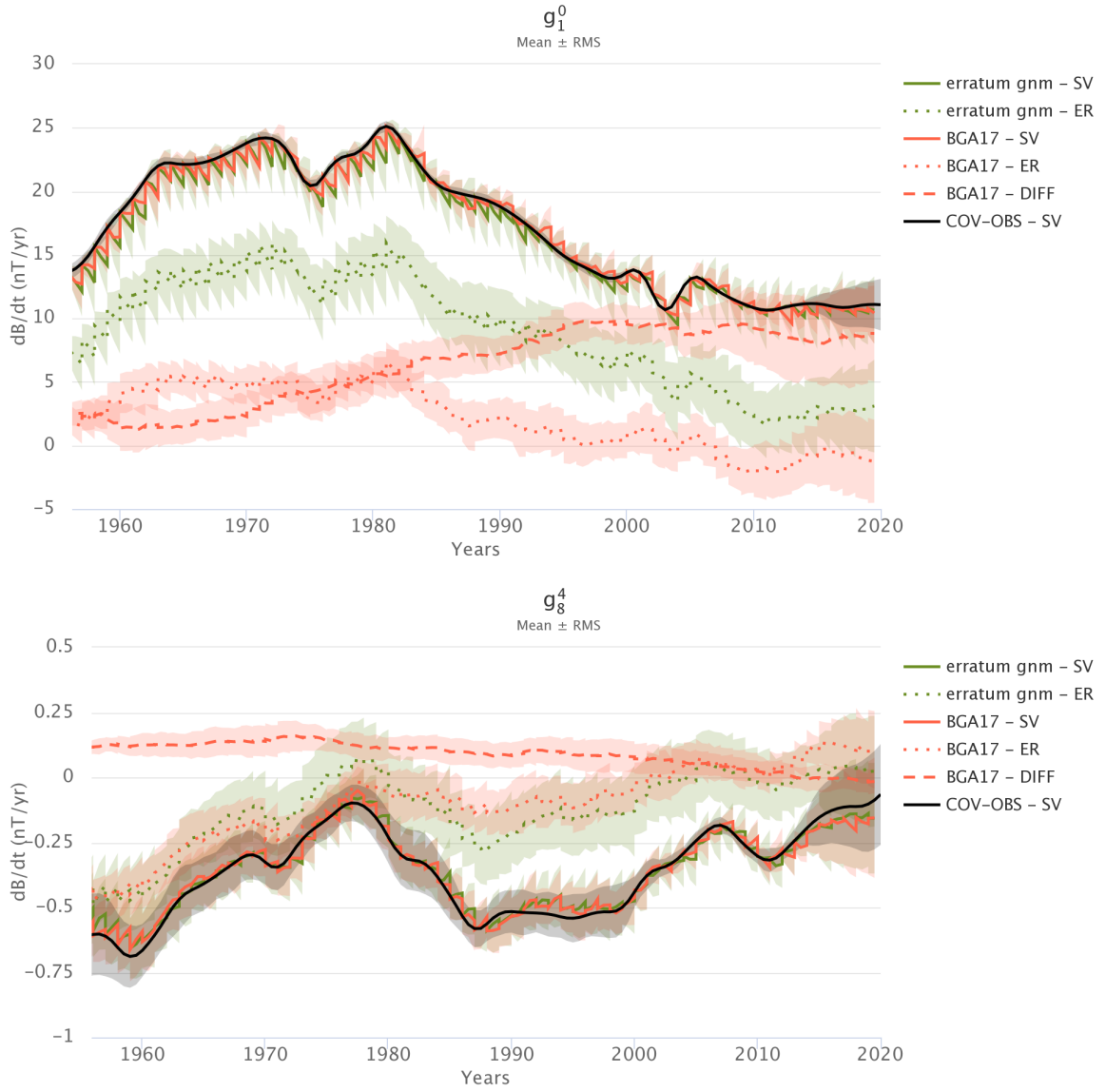

Figure 1. Examples of SV coefficient time series: the COV-OBS.x1 model (Gillet et al. 2015) used here as observation (black), and predictions using (in red) the BGA17 configuration and (in green) the revised approach of the present erratum. In dashed lines the contributions from $\mathbf{d}$ (for BGA17 only). In dotted lines the contributions from $\mathbf{e}$ (for BGA17) and from $\mathbf{e} + \mathbf{d}$ (present erratum). Shaded areas represent the $\pm 1\sigma$ dispersion within the ensemble of realizations.

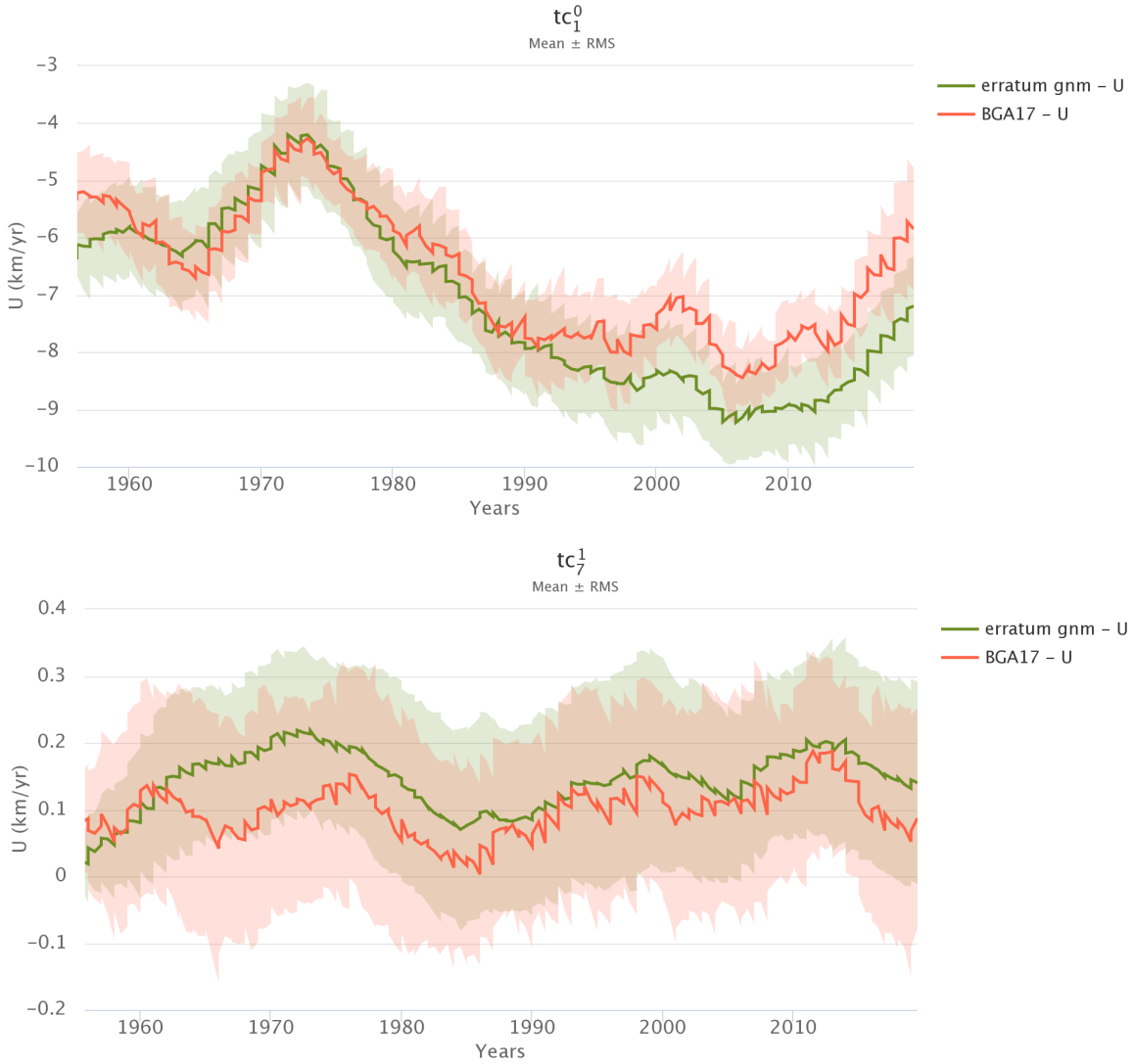

Figure 2. Example of core flow Gauss coefficient time series for the re-analysis in the BGA17 configuration (red) and in the configuration of the present erratum (green). Shaded areas represent the $\pm 1\sigma$ dispersion within the ensemble of realizations.

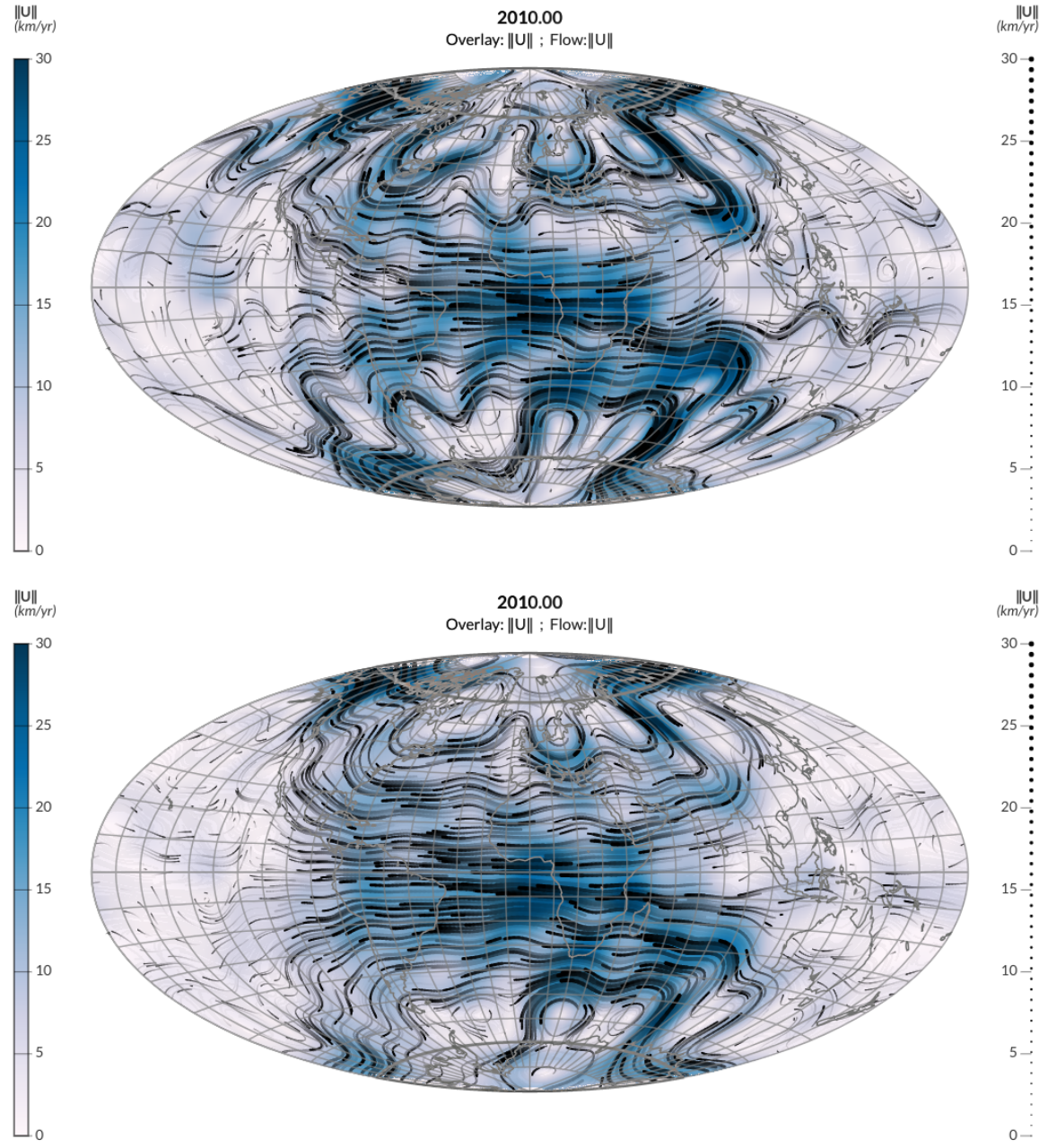

Figure 3. CMB maps of core motions (colorscale: velocity norm; stream-lines in black) in 2010 for the re-analysis in the BGA17 configuration (top) and in the configuration of the present erratum (bottom).

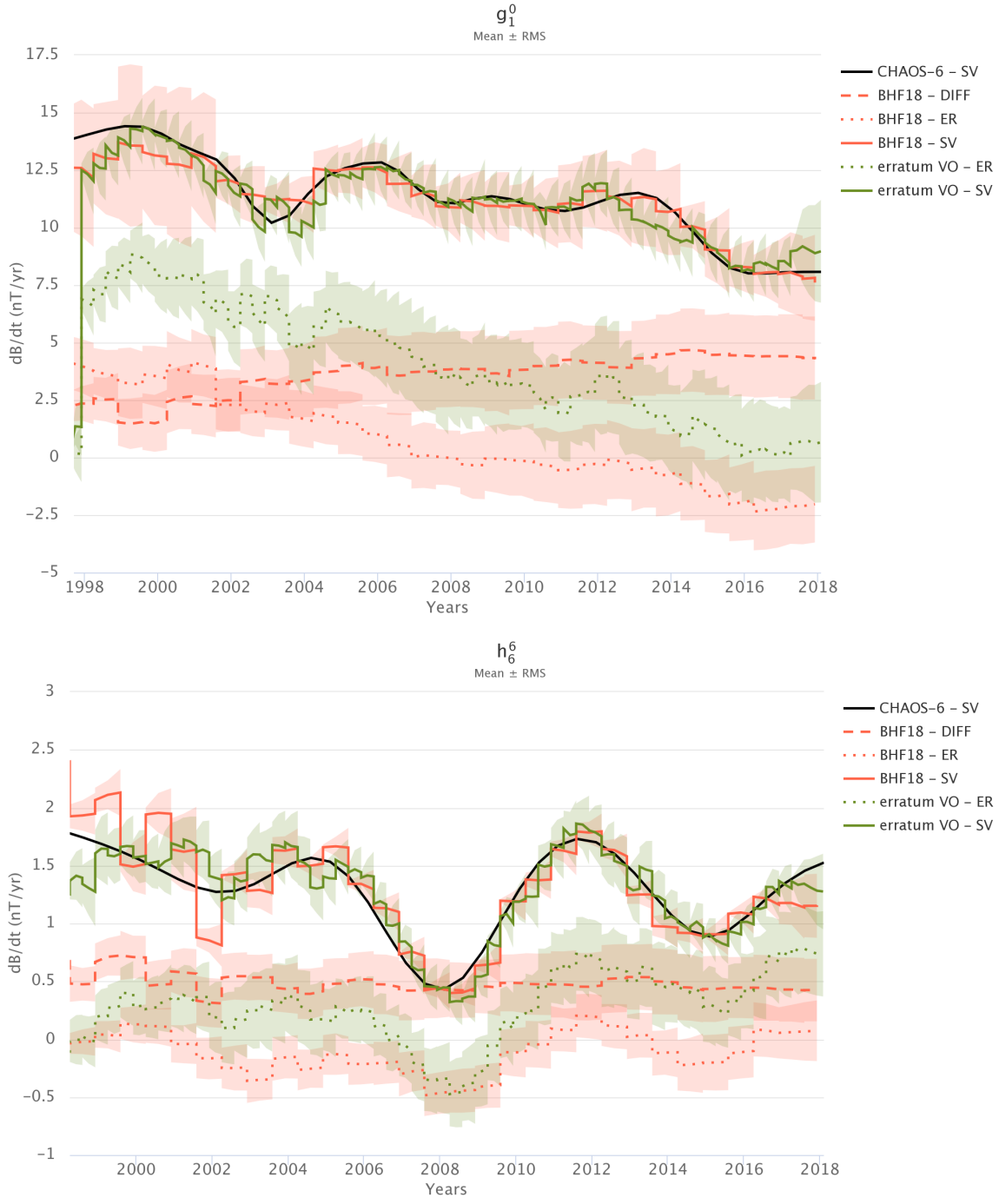

Figure 4. Example of SV coefficient time series for predictions using the BHF18 configuration (red) and the configuration of the present erratum (green). The CHAOS-6 model (Finlay et al. 2016b) is shown in black for comparison. In dashed lines the contributions from $\mathbf{d}$ (for BHF18 only). In dotted lines the contributions from $\mathbf{e}$ (for BHF18) and from $\mathbf{e} + \mathbf{d}$ (present erratum). Shaded areas represent the $\pm 1\sigma$ dispersion within the ensemble of realizations.

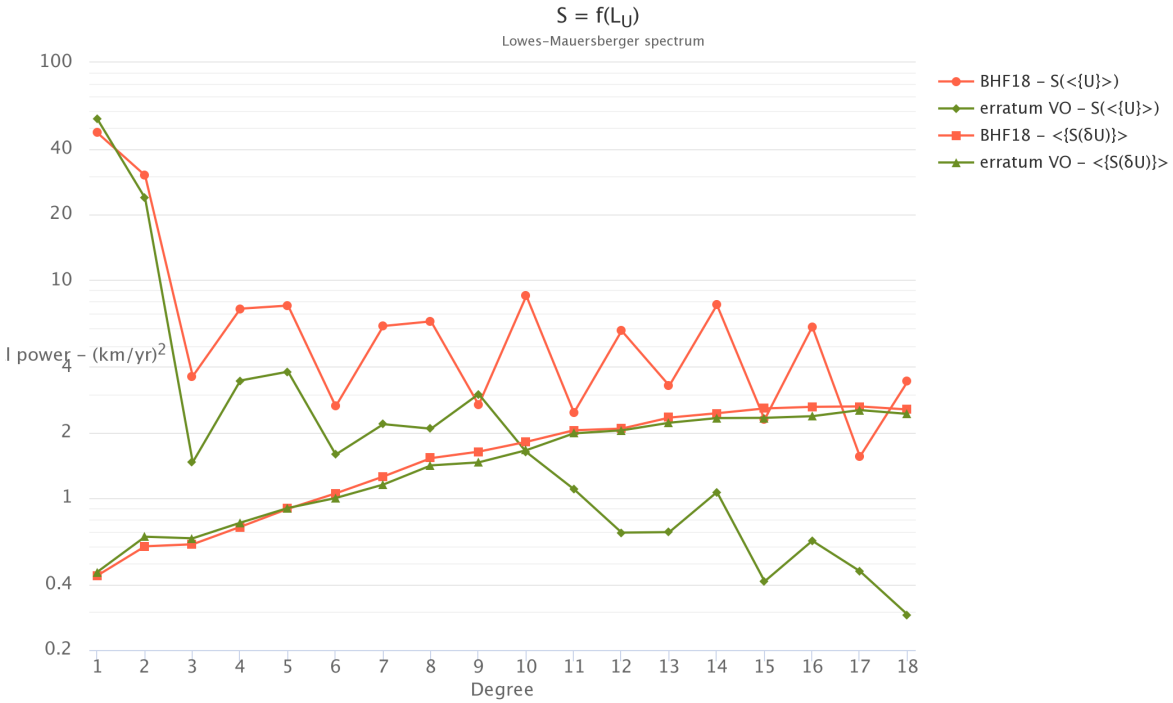

Figure 5. Core flow spectra from BHF18 (red) and from the revised calculations of the present erratum (green), for the ensemble average flow and the dispersion within the ensemble of realizations.

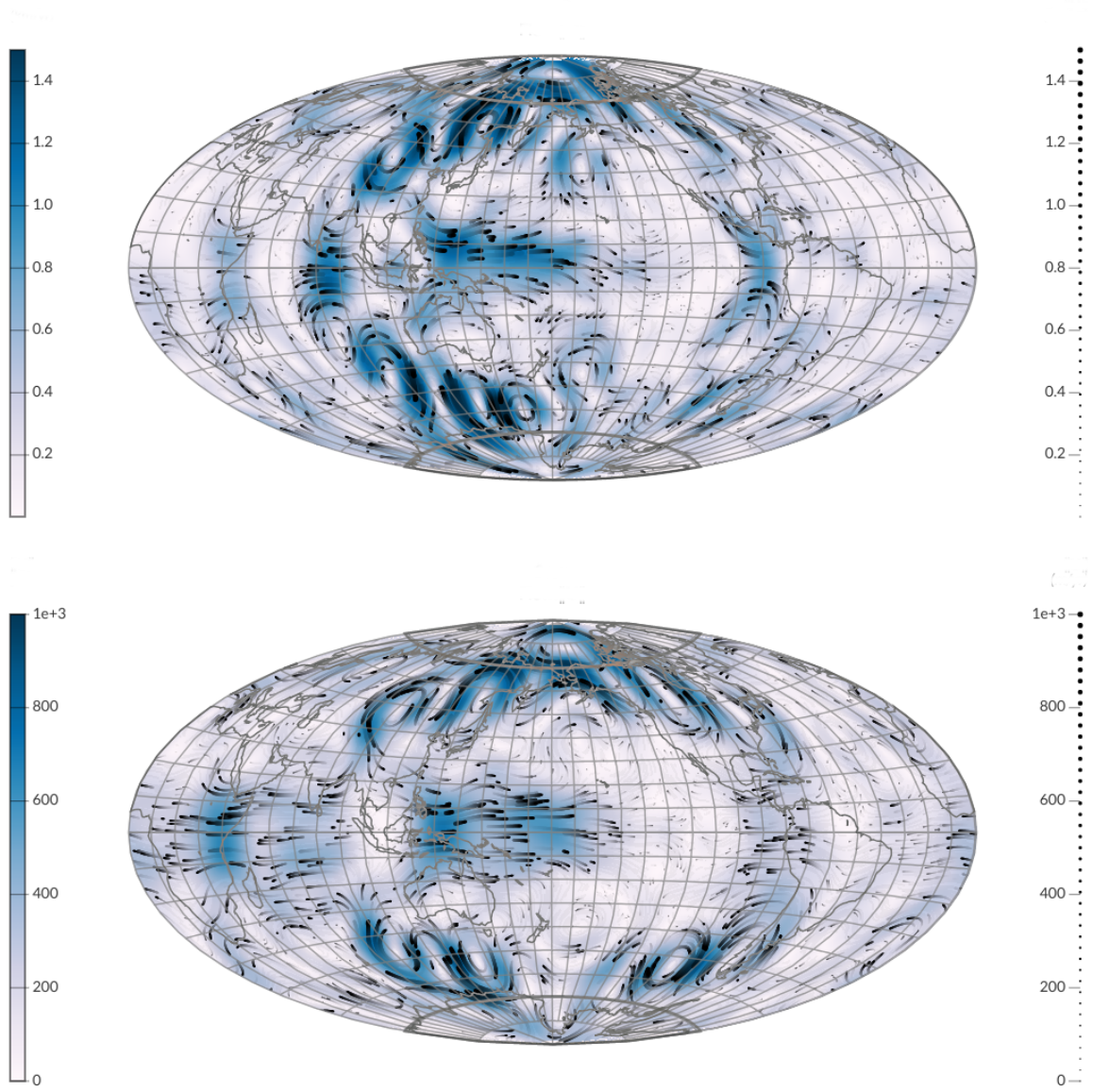

Figure 6. CMB maps of the flow linear acceleration (colorscale: acceleration norm; acceleration stream-lines in black) over the VO+GO era, from the study of BHF18 (top, in km/yr^2) and from the revised calculations of the present erratum (bottom, in m/yr^2) – for the ensemble average flow. Note the different colorscales.